

# Damage analysis of carbon nanofiber modified flax fiber composite by acoustic emission

Dongsheng Li\*, Junbo Shao, Jinping Ou and Yanlei Wang

School of Civil Engineering, Dalian University of Technology, Dalian 116024, China

(Received August 2, 2016, Revised November 1, 2016, Accepted November 3, 2016)

**Abstract.** Fiber reinforced polymer (FRP) has received widespread attention in the field of civil engineering because of its superior durability and corrosion resistance. This article presents the damage mechanisms of a novelty composite called carbon nanofiber modified flax fiber polymer (CNF-modified FFRP). The ability of acoustic emission (AE) to detect damage evolution for different configurations of specimens under uniaxial tension was examined, and some useful AE characteristic parameters were obtained. Test results shows that the mechanical properties of modified composites are associated with the CNF content and the evenness of CNF dispersed in the epoxy matrix. Various damage mechanisms was established by means of scanning electron microscope images. The fuzzy c-means clustering were proposed to classify AE events into groups representing different generation mechanisms. The classifiers are constructed using the traditional AE features -- six parameters from each burst. Amplitude and peak-frequency were selected as the best cluster-definition features from these AE parameters. After comprehensive comparison, a correlation between these AE events classes and the damage mechanisms observed was proposed.

**Keywords:** acoustic emission; flax fiber reinforced polymer; carbon nanofiber; damage mechanisms

## 1. Introduction

Large-scale projects, such as long-span bridges, super-tall buildings, underground structures, and subsea tunnels, have high strength and durability requirements for building materials because these projects are usually undertaken in hostile environments. The civil engineering searches for new building materials constantly to replace traditional reinforced concrete (RC) material. Fiber reinforced polymer (FRP) is a promising material with good properties, such as excellent corrosion resistance, high specific strength and stiffness, as well as outstanding fatigue behavior (Coelho, Sena-Cruz *et al.* 2015, Hollaway 2010). Currently, FRP has been widely applied in structural repairment and strengthening (Kara, Ashour *et al.* 2015, Yu and Kodur 2014). Although FRP has several superior mechanical properties, this material is brittle given that failure would occur directly with a small deformation when its tensile strength is reached. Many researchers are attempting to improve the mechanical performance of FRP. At present, a few studies have shown that carbon nanofiber (CNF) can strengthen epoxy resin matrix, and a very small amount of CNF can improve the mechanical properties of composite materials significantly (Mahfuz, Adnan *et al.* 2004). Allaoui, Bai *et al.* (2002) added some carbon nanotubes to epoxy resin matrix, and their study found that the mechanical properties of epoxy has increased substantially after adding a certain amount of carbon nanotubes (1~4wt%). What's more, CNF can also improve the

durability of composite materials because of its high hydrophobic and good barrier properties (Prolongo, Gude *et al.* 2012). These properties are particularly important for the application of FRP in the civil engineering field.

The ultimate strength of modified composite has a close relationship with CNF content. Most researchers focused on investigating the mechanical behavior of such material. However, studies on the characterization and identification of failure mechanisms of CNF-modified FFRP during tensile testing have not been reported in literature to date. And mechanical testing was measured considering the capacity only. The information of failure and damage evolution was neglected in determining what CNF content was adopted. Typical methods for characterizing failure mechanisms are X-ray and scanning electron microscope (SEM). Another method that may be used to quantitatively characterize and identify the failure mechanisms of CNF-modified FFRP composites is acoustic emission (AE) technique, which is a real-time monitoring method and a non-destructive testing technique. This technique is based on the detection of transient elastic waves produced by internal micro placement because of plastic deformation or cracks propagation. Many studies have proven that AE is a very useful technique to detect and evaluate the failure process of composite material (Karimi, Heidary *et al.* 2012, Kempf, Skrabala *et al.* 2014). The present study aims to investigate the damage mechanism of flax fiber composite plates under uniaxial tension using AE technique. During the test, the AE system showed a few characteristic parameters, such as AE hits, peak-frequency and amplitude. These parameters can help to describe the failure mechanism of a material efficiently. The failure mechanisms of metallized glass fiber-reinforced epoxy

---

\*Corresponding author, Ph.D.  
E-mail: lidongsheng@dlut.edu.cn

Table 1 AE characteristics of the main damage mechanisms in the literature

AE feature	Matrix cracking	Debonding	Fiber pull-out	Fiber breakage	Material	Reference
Amplitude (dB)	40-50 40-50	45-60 50-60	60-80 55-75	80-96 >80	Flax/LPET Flax/resin	Aslan (2013) Monti, El Mahi <i>et al.</i> (2016)
Peak frequency (kHz)	90-180 0-50	240-310 200-300	180-240 500-600	>300 400-500	CFRP/epoxy CFRP/epoxy	De Groot, Wijnen <i>et al.</i> (1995) Gutkin, Green <i>et al.</i> (2016)

composites under tensile loading were identified successfully using AE analysis (Njuhovic, Bräu *et al.* 2015). Each AE event can be considered as a signature of one of different damage modes for cluster algorithm (Huguet, Godin *et al.* 2002). Aslan (2013) and Monti, El Mahi *et al.* (2016) utilized time domain features (amplitude, duration, rise time, counts, and energy) and found that damage mechanisms are highly correlated with amplitude. Many others found that peak-frequency can be regarded as the best AE descriptor for damage characterization, whereas there is an obvious overlap for other parameters (Gutkin, Green *et al.* 2011). Table 1 summaries damage mode links to AE features proposed by different authors. In the latest literature (Li, Lomov *et al.* 2014, 2015), damage modes were determined by AE events combining amplitude and peak-frequency, and AE events are classified into low frequency/low amplitude, low frequency/high amplitude and high frequency clusters.

The present study focuses on identifying the failure mechanisms of CNF-modified FFRP under uniaxial tension using AE analysis. A few representative features, such as cumulative AE hits, amplitude and peak-frequency, were extracted to determine their failure modes. Furthermore, the comparative analysis on the AE signal difference of specimens were conducted. Assessment and analysis proved that the mechanical properties of CNF-modified FFRP composite are closely related to the content of CNF in the matrix.

## 2. Experimental procedure

### 2.1 Material characteristics

The epoxy resin adopted in the experiment is a special resin called SWANCOR 2511-1A/BS, which is produced by Swancor Wind Blade Materials Co., Ltd., China. The detailed parameters are shown in Table 2. The type of CNF is PR-24-XT-HHT, which is manufactured by Pyrograf Products Inc., USA. The diameter of PR-24-XT-HHT is 100 nm and the length is 50~200  $\mu\text{m}$ . In consideration of its environmental friendliness, low cost and superior performance, we chose flax fiber to replace the traditional fiber as the reinforced fiber of the composites in this test. Table 3 lists the unidirectional mechanical performance of flax fiber.

Table 2 Physical properties of the epoxy resin

Type	SWANCOR 2511-1 A	SWANCOR 2511-1 BS
Viscosity (cps, 25°C)	900~1300	10~50
Density (g/cm <sup>3</sup> , 25°C)	1.1~1.2	0.9~1.0
weight ratio		100:30
Tg(°C)		80~90

Table 3 Unidirectional mechanical performance of flax fiber

Density (g/cm <sup>3</sup> )	Tensile strength (MPa)	E-modulus (GPa)	Elongation at failure (%)	Thickness (mm)
1.4	800~1500	60~80	1.2~1.6	0.16

### 2.2 Specimen preparation

In this work, the modified epoxy (CNF/epoxy) was prepared at first. High-speed mixer, ultrasonic dispersion and vacuum were used to disperse the CNF evenly in the epoxy matrix. The CNF were first added to the SWANCOR 2511-1A resin and hand-stirred. Then, the mixture was stirred in a blender at a high speed of 2000r/min for 30 min. Whereafter, the mixture was sonicated in a temperature-controlled sonicator at 60°C. Then the curing agent SWANCOR

2511-1BS was added and mixed by blender for 5min. The mixture was finally placed in a vacuum chamber for 20 min to remove air bubbles. Thus the CNF/epoxy matrix was well prepared. The flax laminates were made by hand lay-up method. Flax laminates adopted the form of a sandwich, in which both faces of the flax fiber were covered by the epoxy matrix. The schematic of CNF dispersion in composite are shown in Fig. 1. Three types of flax fiber composite plates with different CNF contents in their matrix were tested. For the purpose of matrix cracking studies, corresponding resin specimens were made at the same time. The basic information of these types of specimens is shown in Table 4. The shape and size of the P-type specimens were designed according to ASTM D3039, as shown in Fig. 2. The central measurement range of the test specimens is 100 mm and the width is 25 mm, particularly, 50 mm long end tabs were used to clamp the specimens to the testing

machine. To prevent the end socket of test specimens from fracturing in an untimely manner during the tensile process, four aluminum strengthened sheets were set on both ends of each specimen according to the test method (GB/T 3354-1999) for tensile properties of oriented fiber reinforced plastics.

### 2.3 Experimental setup

The test specimens were fixed on the electronic universal testing machine. Then, sandpaper was used to wipe clean the material surface before conducting tensile test. An extensometer was also set on the specimens to conduct the measurement of tensile strain. According to ASTM D638, the loading process employed the displacement control method with a loading rate of 2mm/min. The loading procedure was continued with increasing load until ultimate failure was reached. The entire damage process of specimens was monitored by using Physics Acoustic Corporation system and AE win software. Two RS-2A resonant sensors (50-400kHz) were respectively pressed onto the two sides of the tensile specimen and were connected to the AE monitor system via a preamplifier. The AE sensor was fixed by a rubber band wrapped around the specimen and sensor. Prior to the experiment, a broken lead experiment was performed to eliminate ambient noise. The basic parameters of AE monitor system were set as follows: the main amplifier gain of AE system was set at 20 dB, preamplifier gain was 40 dB, sample rate was 5 MHz, and a threshold of 40dB used to avoid detecting most noise from the surrounding area. The tensile test of CNF-modified composite plates is shown in Fig. 3.

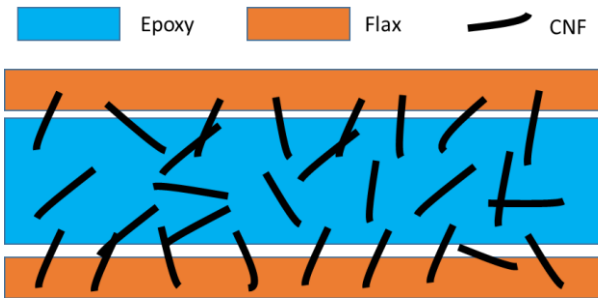


Fig. 1 Schematic of CNF dispersion in composite

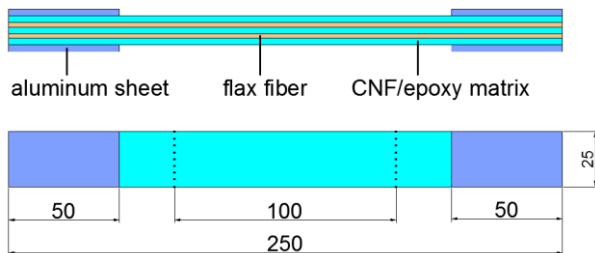


Fig. 2 Shape and size of CNF/ Epoxy/Flax specimens (units:mm)

Table 4 Basic information of specimens

Type	Thickness(mm)	Ingredient	Content of CNF in matrix	Number of test sample
A-0.25	3	CNF/ Epoxy	0.25% wt	3
A-0.5	3	CNF/ Epoxy	0.5% wt	3
A-1.0	3	CNF/ Epoxy	1.0% wt	3
P-0.25	2	CNF/ Epoxy/Flax	0.25% wt	5
P-0.5	2	CNF/ Epoxy/Flax	0.5% wt	5
P-1.0	2	CNF/ Epoxy/Flax	1.0% wt	5



Fig. 3 Experiment loading system

### 3. Fuzzy c-means clustering

Fuzzy c-means (FCM) is a data clustering technique wherein each data point belongs to a cluster to some degree that is specified by a membership grade. This algorithm was first put forward by Jim Bezdek in 1981, as an improvement for traditional hard clustering. The aim of FCM is to find cluster centers  $C_i$  that minimize the function  $J$ : (Bezdek 2013, Marec, Thomas *et al.* 2008)

$$J(U, V) = \sum_{j=1}^n \sum_{i=1}^m [u_i(x_j)]^f d^2(x_j, C_i) \quad (1)$$

Where  $U$  is fuzzy partition matrix with  $m$  lines and  $n$  columns,  $V$  is cluster center matrix.

$$U = \begin{bmatrix} u_1(x_1) & u_1(x_2) & \dots & u_1(x_n) \\ u_2(x_1) & u_2(x_2) & \dots & u_2(x_n) \\ \dots & \dots & \dots & \dots \\ u_m(x_1) & u_m(x_2) & \dots & u_m(x_n) \end{bmatrix} \quad (2)$$

$$V = [C_1 | C_2 | \dots | C_m] \quad (3)$$

In which  $u_i(x_j)$  is the membership value of  $j$ th data point to the  $i$ th cluster, under the condition

$$\sum_{i=1}^m u_i(x_j) = 1 \quad \forall j \quad (4)$$

$f$  is a scalar which represents the fuzzy degree ( $f=2$ ). And  $d^2(x_i, C_i)$  is the distance between the pattern vector  $x_i$  and the cluster center  $C_i$ , usually adopt the square of the Euclidean distance.

$$d^2(x_j, C_i) = \sqrt{\sum_{j=1}^m (x_{kj} - v_{ij})^2} \quad (5)$$

In order to determine the appropriate number of clusters in the data set, the most popular validity criteria for fuzzy clustering is adopt: Xie and Beni's Index ( $XB$ ). It aims to quantify the ratio of the total variation within clusters and the separation of clusters (Xie and Beni 1991). The optimal number of clusters should minimize the value of the index. It is defined as follows

$$XB(c) = \frac{\sum_{i=1}^c \sum_{j=1}^N (u_i(x_j))^m \|x_j - v_i\|^2}{N \min_{i \neq j} \|v_j - v_i\|^2} \quad (6)$$

## 4. Experimental results and discussion

### 4.1 AE parameter analysis and the explanation of SEM

Table 4 lists the mechanical properties of test specimens. P-0.5 has the highest tensile strength and modulus, followed by P-1.0 and P-0.25 as the lowest. This illustrates that 0.5 wt% CNF content has the best improvements effect on this improved composites in this experiment. Similar result has been reported in (Xiao, Song *et al.* 2015). In order to verify the results, SEM images of the failure surface of CNF-modified composites were applied. It should be noted that enhancement effect depends on the modified epoxy matrix. SEM images of the fracture section of A-type specimens are shown in Fig. 6. Joint surface increased with the raise of CNF content. The increased surface roughness implies that the path of the crack tip was distorted because of the carbon nanofiber. Actually, the essence of this modified material is closely related to the fiber-bridging as elaborated in (Tsantzalis, Karapappas *et al.* 2007). The fiber-bridging is the major energy absorbing mechanisms. Therefore, cracking resistance was improved significantly and the mechanical properties of modified composites strengthened accordingly. However, the performance of the composite material is associated with the CNF content, and is affected by the evenness of CNF dispersed in the epoxy matrix (Xiao, Song *et al.* 2015, Zhou, Pervin *et al.* 2008). When the CNF concentration was 1 wt%, a portion of CNF in the epoxy resin matrix began to agglomerate as shown in Fig. 7(d). The crack initiation was caused by the stress

concentrations resulted from the agglomerated CNFs, thereby deteriorating the mechanical performance of the composites. This reason explains why P-0.5 possessed the best mechanical properties.

The AE hits is defined as the number of signals collected by AE sensor and could indicate the damage condition of material in real-time. Testing results showed that the variation trend of AE activity was similar to that of a specimen of the same type. Therefore, the AE analysis results of only three typical specimens were shown in this paper. Fig. 4 shows the relationship between stress and cumulative hits under uniaxial loading. With the increase of load, the curve of hits increase continuously and the damage get further intensified. There are two noticeable locations of slope change in the curve of cumulative hits. The first slope change is at low stress level, the AE generation mechanism is attributed to matrix cracking and the internal defects such as microvoid and bubble. Subsequently, a slow increase of AE hits imply that the composites turned into a relatively stable state. Prior to the final failure (90% ultimate strength), the rate of AE hits rose significantly again. Noticed that P-0.5 primarily discriminates with the other two specimens in the distribution of AE hits. Few damage signals of P-0.5 were recorded in the initial stage and most of damage occurred in the final failure stage. This may indicate that the matrix of P-0.5 has the least defects and the mechanical properties obtained a significant improvements. And a considerable number of AE hits was detected in P-1.0 during the initiation of loading. The causes of this phenomenon is evident, that is agglomerated CNFs. The rate of AE hits showed high sensitivity to the damage evolution of modified composite. And the AE results agreed with the microscopic analyses well.

Further investigation was conducted to identify the failure mechanisms of CNF-modified FFRP. In terms of composite materials, the damage modes mainly include matrix cracking, interface debonding, fiber pull-out and fiber breakage. Fig. 7 presents the fracture sectional SEM images of P-type specimens after breakage. At a macroscopic scale, the observations of these failure profiles provided brought a lot of information. And all these damage modes were also observed. Peak-frequency analysis is one of the promising techniques to discriminate these failure modes. Classifications of failure modes based on the frequency of AE signals have been investigated. Fiber breakage in the high frequency range and interface debonding in the intermediate frequency range. Matrix cracking is usually identified to the low frequency range, while fibre pull-out have a frequency range between debonding and fiber fracture (De Groot, Wijnen *et al.* 1995, Gutkin, Green *et al.* 2011). Fig. 5 shows the variation of peak-frequency with time for the specimen subjected to tensile test with AE monitoring. Two remarkable ranges of peak frequency are identified. With few exceptions, the frequency band of A-type specimens almost located between 0 and 200 kHz. Since the damage mode of A-type specimens is single. This illustrates matrix-cracking (blue dot) is identified to the low frequency range. However, it seems that the frequency band of another three damage modes (red dot) are mixed together. It is difficult to

discriminate each damage mode directly only rely on the distribution of peak-frequency. Thus, a multi-parameter clustering analysis would be carried out in the following section.

Table 5 Mechanical properties of FFRP with different contents

Specimen	Tensile strength (MPa)	Elasticity modulus (GPa)	Elongation at break (%)
P-0.25	177.46 ± 5.23	15.39 ± 0.98	1.76 ± 0.10
P-0.5	195.01 ± 4.06	17.42 ± 1.21	2.03 ± 0.09
P-1.0	185.24 ± 6.89	15.89 ± 1.73	1.84 ± 0.13

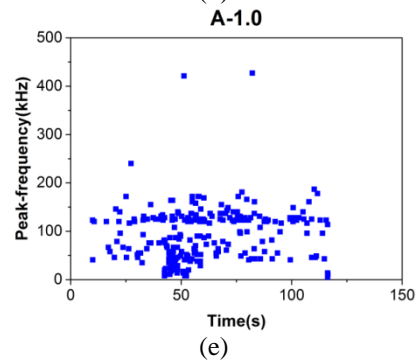
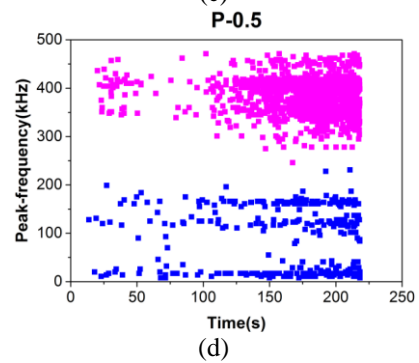
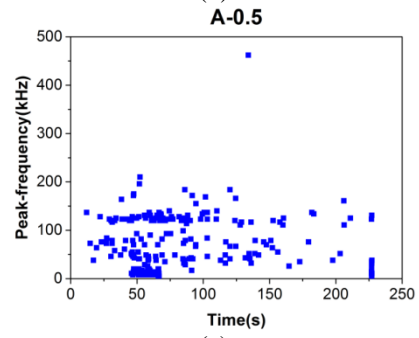
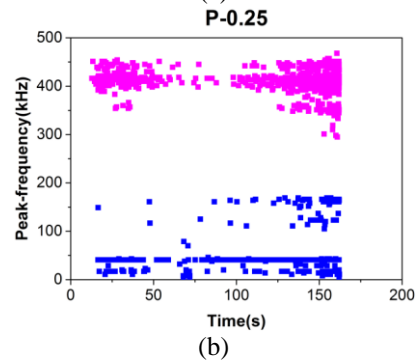
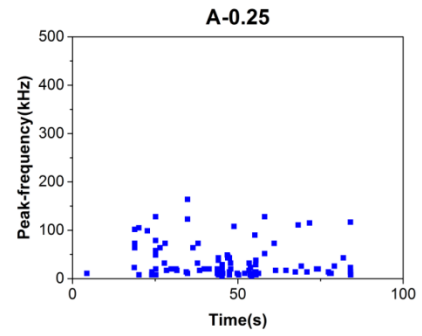
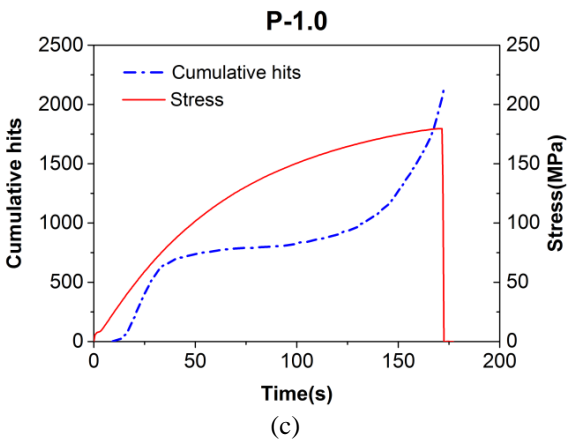
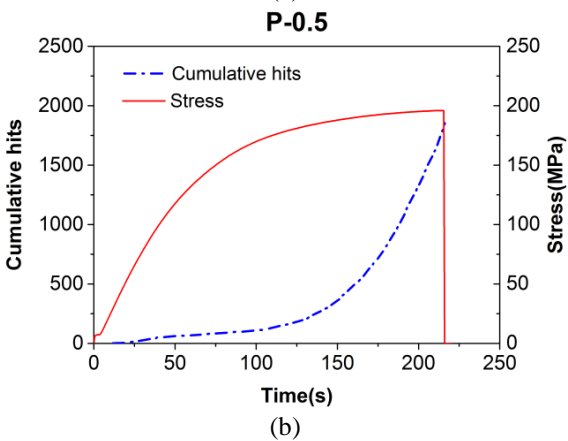
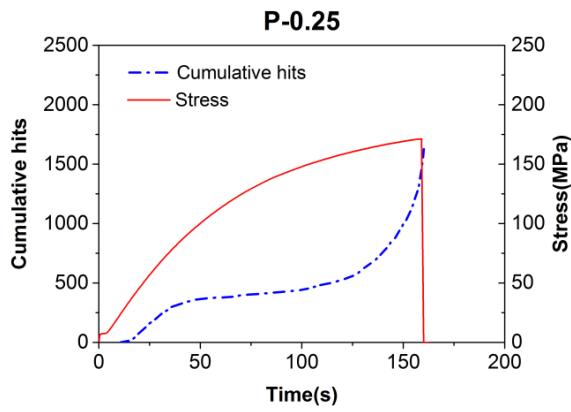


Fig. 4 Cumulative hits and stress versus time

Continued-

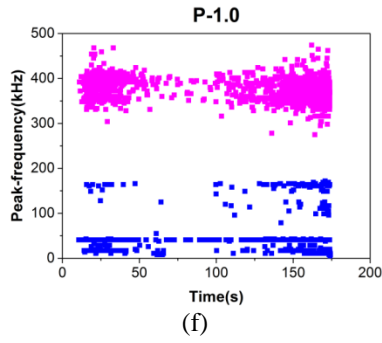
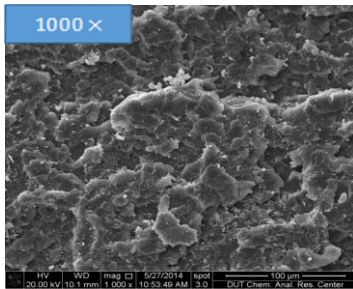
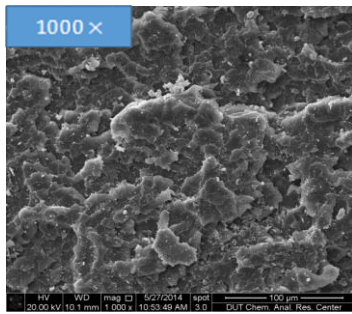


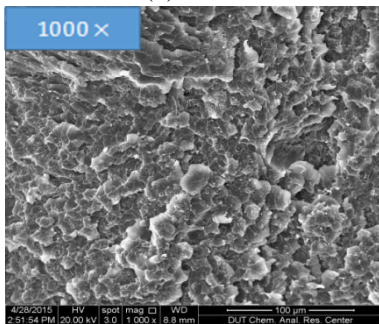
Fig. 5 Peak-frequency versus time



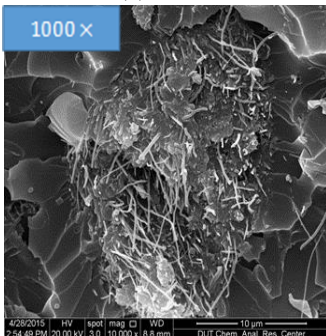
(a) A-0.25



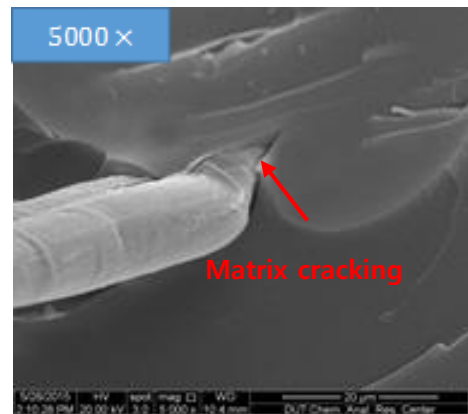
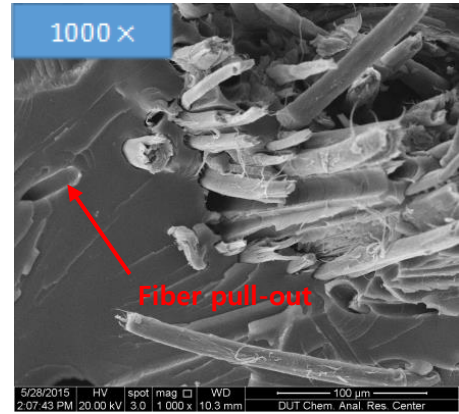
(b) A-0.5



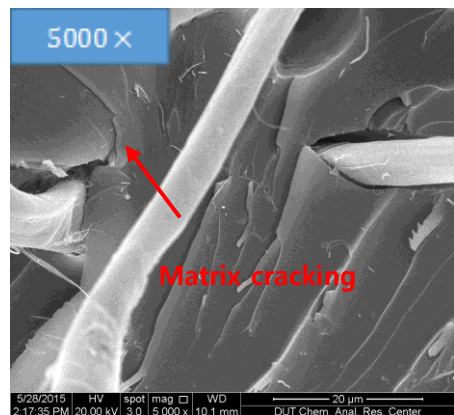
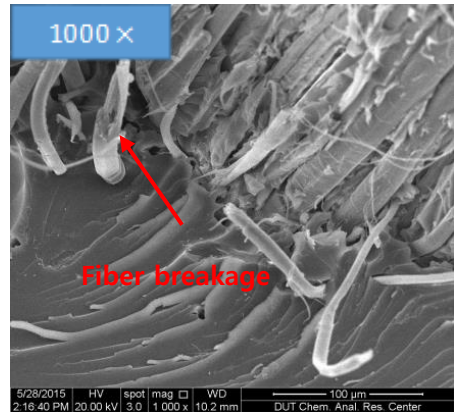
(c) A-1.0



(d) A-1.0 (bad dispersed)



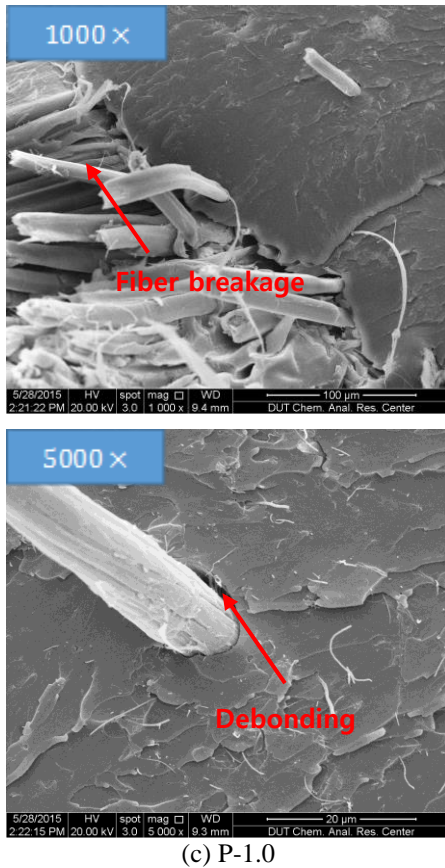
(a) P-0.25



(b) P-0.5

Continued-

Fig. 6 SEM images of fracture area in A-type specimen



(c) P-1.0

Fig. 7 SEM images of fracture area in P-type specimen

#### 4.2 Damage identification based on cluster results

In cluster analysis, feature selection is a vital procedure and the choice of cluster parameter can influence the validity of cluster to some extent. The cluster parameter should include as much descriptive information as possible and remove the irrelevant messages. Six basic parameters of the AE signals were selected to describe an AE signal: risetime, counts, energy, duration, amplitude and peak-frequency. Each descriptor is normalized to range from 0 to 1 before data analysis. Then, a six-component descriptor vector represents each typical AE signal. The index of cluster validity used is Xie and Beni's (*XB*) index, as defined in Eqs. (6). The number of cluster *k* is calculated using the range from 2 to 10. Fig. 7 shows the number of clusters evaluated by *XB* Index. The minimum of *XB* Index indicates the optimal number of clusters. The optimal number of clusters for three typical specimens is marked by a red rectangle. Therefore four is chosen as the cluster number for analysis of all the data sets. The application of the classification methodology returned the following results. Fig. 8(a) presents the amplitudes of these AE classes with respect to the time. After comparison and identification, AE events present a best separation in the space of amplitude and peak-frequency, as shown in Fig. 8(b). This outcome indicates that peak-frequency and amplitude are the most appropriate to discriminate different damage modes. This result is consistent with the recent researches (Li, Lomov *et al.* 2014, 2015).

To primarily correlate the resulted clusters with different damage mechanisms, four clusters were compared with amplitude distribution and peak-frequency band. Based on previous analyses, CL1 and CL2 with peak-frequency range 0-200 kHz can be attributed to matrix-cracking. According to the literature as mentioned in Table 1, AE bursts caused by fiber/matrix debonding usually possess a lower amplitudes than those of fiber pull-out (Aslan 2013, Monti, El Mahi *et al.* 2016). Furthermore, the number of CL4 is much less than that of CL3 and the occurrence of CL4 is largely at a high stress level. As a consequence, CL3 with amplitude distribution 40-50 dB relates to fiber/matrix debonding. While AE events in CL4 have higher amplitude and similar frequency distribution with CL3, possibly associate with fiber pull-out. A small part of fiber breakage may mix in CL4, but the clustering algorithm fail to isolate fiber breakage because of its exiguity. The boundaries of the clusters are summarized in Table 7. Fig. 9 presents the cumulative hits for each class with respect to time during tensile process. This is a good indication of AE events evolution. A significant increase of each class is observed just before failure. And it is interesting to observe considerable CL4 events of P-1.0 appeared in elastic stage. The presence of large porosity regions (cavity among fibres) weakens transmitting the load sharing between fiber and matrix (Aslan 2013), therefore more fiber damage was detected accordingly. With the characteristic descriptors, the AE classification procedure is efficient to identify damage mechanisms occurring during tensile tests.

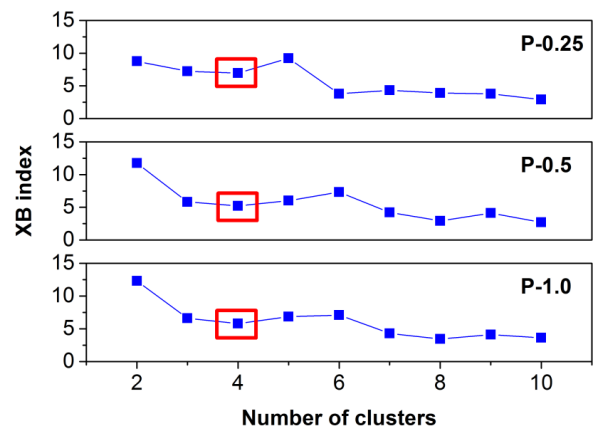
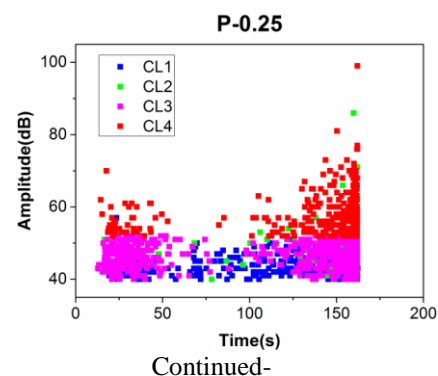


Fig. 8 The number of clusters evaluated by Xie and Beni's Index



Continued-

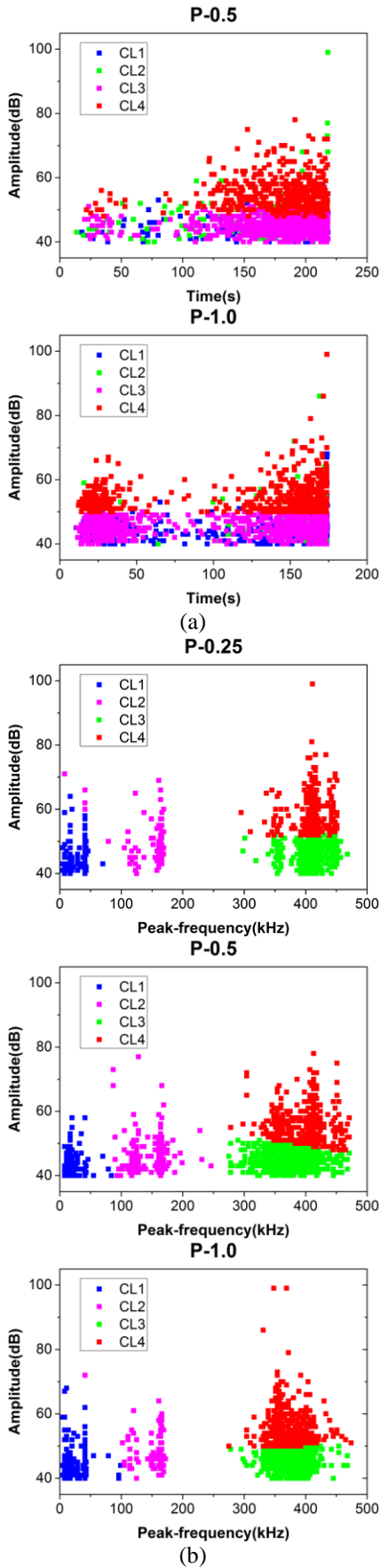


Fig. 9 Typical AE registration by FCM cluster algorithm

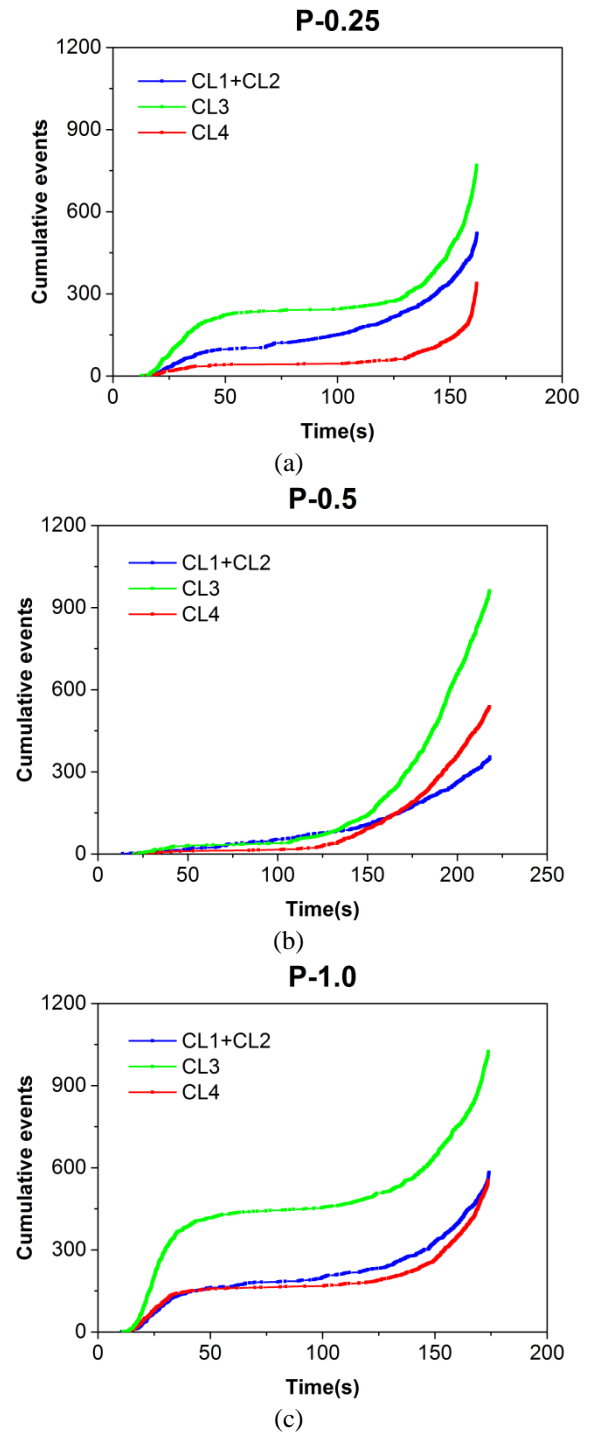


Fig. 10 AE events progression of different clusters

Table 7 Cluster bounds of P-type specimen

Cluster	Amplitude (dB)	Peak-frequency (kHz)
CL1+CL2	40-80	0-200
CL3	40-50	300-500
CL4	>50	300-500

## 5. Conclusions

CNF was used to improve the mechanical properties of epoxy resin and flax/epoxy composites. The mechanical properties of modified composites are associated with the CNF content and the evenness of CNF dispersed in the epoxy matrix. When the concentration of CNF is 1 wt%, CNF in the epoxy matrix agglomerates gradually. Thus, 0.5 wt% CNF content has the best improvements effect on this improved composites in this experiment. The damage evolution and failure mechanisms of CNF-modified FRP were investigated on the basis of the measured AE characteristic from the present experimental testing and analysis results. The rate of AE hits showed high sensitivity to the damage evolution of modified composite. Cumulative AE hits in initial stage could reflect the number of internal defects to some extent. P-0.5 has a significant difference with the other two specimen on the distribution of AE signal. Different CNF content may lead to different mechanical properties, and different mechanical properties may bring about different AE results. It turns out that amplitude and peak-frequency are the most important parameters in this discrimination. The correspondence between the AE events in the clusters and the damage mode can be hypothesized, based on literature data, as follows: CL1 and CL2 -- matrix cracking, CL3 -- fiber/matrix debonding, CL4 -- fiber pull-out and fiber breakage. This correspondence should be further confirmed and detailed in the future work.

## Acknowledgements

The authors are grateful for the financial support from National Natural Science Foundation of China (NSFC) under Grant Nos. 51278083, 51478079, and the Fundamental Research Funds for the Central Universities (Project No. DUT15LAB11).

## References

- Allaoui, A., Bai, S., Cheng, H.M. and Bai, J.B. (2002), "Mechanical and electrical properties of a MWNT/epoxy composite", *Compos. Sci. Technol.*, **62**(15), 1993-1998.
- Aslan, M. (2013), "Investigation of damage mechanism of flax fibre LPET commingled composites by acoustic emission", *Compos. Part B: Eng.*, **54**, 289-297.
- Bezdek, J.C. (2013), *Pattern recognition with fuzzy objective function algorithms*, Springer Science & Business Media.
- Coelho, M.R., Sena-Cruz, J.M. and Neves, L.A. (2015), "A review on the bond behavior of FRP NSM systems in concrete", *Constr. Build. Mater.*, **93**, 1157-1169.
- De Groot, P.J., Wijnen, P.A. and Janssen, R.B. (1995), "Real-time frequency determination of acoustic emission for different fracture mechanisms in carbon/epoxy composites", *Compos. Sci. Technol.*, **55**(4), 405-412.
- Gutkin, R., Green, C.J., Vangrattanachai, S., Pinho, S.T., Robinson, P. and Curtis, P.T. (2011), "On acoustic emission for failure investigation in CFRP: Pattern recognition and peak frequency analyses", *Mech. Syst. Signal Pr.*, **25**(4), 1393-1407.
- Hollaway, L.C. (2010), "A review of the present and future utilisation of FRP composites in the civil infrastructure with reference to their important in-service properties", *Constr. Build. Mater.*, **24**(12), 2419-2445.
- Huguet, S., Godin, N., Gaertner, R., Salmon, L. and Villard, D. (2002), "Use of acoustic emission to identify damage modes in glass fibre reinforced polyester", *Compos. Sci. Technol.*, **62**(10), 1433-1444.
- Karimi, N.Z., Heidary, H. and Ahmadi, M. (2012), "Residual tensile strength monitoring of drilled composite materials by acoustic emission", *Mater. Des.*, **40**, 229-236.
- Kara, I.F., Ashour, A.F. and Köroğlu, M.A. (2015), "Flexural behavior of hybrid FRP/steel reinforced concrete beams", *Compos. Struct.*, **129**, 111-121.
- Kempf, M., Skrabala, O. and Altstädt, V. (2014), "Acoustic emission analysis for characterisation of damage mechanisms in fibre reinforced thermosetting polyurethane and epoxy", *Compos. Part B: Eng.*, **56**, 477-483.
- Li, L., Lomov, S.V., Yan, X. and Carvelli, V. (2014), "Cluster analysis of acoustic emission signals for 2D and 3D woven glass/epoxy composites", *Compos. Struct.*, **116**, 286-299.
- Li, L., Lomov, S.V. and Yan, X. (2015), "Correlation of acoustic emission with optically observed damage in a glass/epoxy woven laminate under tensile loading", *Compos. Struct.*, **123**, 45-53.
- Mahfuz, H., Adnan, A., Rangari, V.K., Jeelani, S. and Jang, B.Z. (2004), "Carbon nanoparticles/whiskers reinforced composites and their tensile response", *Compos. Part A: Appl. Sci. Manufact.*, **35**(5), 519-527.
- Marec, A., Thomas, J.H. and El Guerjouma, R. (2008), "Damage characterization of polymer-based composite materials: Multivariable analysis and wavelet transform for clustering acoustic emission data", *Mech. Syst. Signal Pr.*, **22**(6), 1441-1464.
- Monti, A., El Mahi, A., Jendli, Z. and Guillaumat, L. (2016), "Mechanical behaviour and damage mechanisms analysis of a flax-fibre reinforced composite by acoustic emission", *Compos. Part A: Appl. Sci. Manufact.*, **90**, 100-110.
- Njuhovic, E., Bräu, M., Wolff-Fabris, F., Starzynski, K. and Altstädt, V. (2015), "Identification of failure mechanisms of metallised glass fibre reinforced composites under tensile loading using acoustic emission analysis", *Compos. Part B: Eng.*, **81**, 1-13.
- Prolongo, S.G., Gude, M.R. and Urena, A. (2012), "Water uptake of epoxy composites reinforced with carbon nanofillers", *Compos. Part A: Appl. Sci. Manufact.*, **43**(12), 2169-2175.
- Ramirez-Jimenez, C.R., Papadakis, N., Reynolds, N., Gan, T.H., Purnell, P. and Pharaoh, M. (2004), "Identification of failure modes in glass/polypropylene composites by means of the primary frequency content of the acoustic emission event", *Compos. Sci. Technol.*, **64**(12), 1819-1827.
- Tsantzalis, S., Karapappas, P., Vavouliotis, A., Tsoira, P., Kostopoulos, V., Tanimoto, T. and Friedrich, K. (2007), "On the improvement of toughness of CFRPs with resin doped with CNF and PZT particles", *Compos. Part A: Appl. Sci. Manufact.*, **38**(4), 1159-1162.
- Xie, X.L. and Beni, G. (1991), "A validity measure for fuzzy clustering", *IEEE T. Pattern Anal.*, **13**(8), 841-847.
- Xiao, H., Song, G., Li, H. and Sun, L. (2015), "Improved tensile properties of carbon nanotube modified epoxy and its continuous carbon fiber reinforced composites", *Polymer Compos.*, **36**(9), 1664-1668.
- Yu, B. and Kodur, V.K.R. (2014), "Fire behavior of concrete T-beams strengthened with near-surface mounted FRP reinforcement", *Eng. Struct.*, **80**, 350-361.
- Zhou, Y., Pervin, F., Jeelani, S. and Mallick, P.K. (2008), "Improvement in mechanical properties of carbon fabric-epoxy composite using carbon nanofibers", *J. Mater. Process.*

